

# Hydro-elastic analysis of a propeller using CFD and FEM co-simulation

Vesa Nieminen<sup>1</sup>

<sup>1</sup>VTT Technical Research Centre of Finland, Espoo, Finland

## ABSTRACT

This paper presents a two-way Fluid-Structure Interaction (FSI) co-simulation of a marine propeller under operational loading. The case of study was the quasi-static elastic response of Marintek propeller P1374 in a steady flow condition. A two-way FSI co-simulation with the Fluent CFD-code and the Abaqus structural FE-code utilizing MpCCI interface was applied successfully. The so-called weak coupling was used, which means that each problem is solved separately and during each time step some variables are exchanged and inserted into the equations of the other problem. The results were compared with experimental data, which had been published earlier.

Agreement between calculated and measured thrust and torque coefficients was good. The order of magnitude of blade displacements corresponded to the measured ones. However, the simulated twist of the blade was smaller than the measured one. Also the simulated modifications to the performance characteristics were smaller than the measured ones. One possible reason for this can be the uncertainties in material properties of the blade. The measured propeller had been 3D printed in plastic, which may have impact on the material properties.

## Keywords

Fluid-Structure Interaction, Co-simulation, CFD, FEM

## 1 INTRODUCTION

For standard metallic propellers in common operations the elasticity of the blades is not a major concern. However, hydroelastic response of the propeller blades became of interest in conjunction with the attempts of using composite materials to obtain flexible blades that would assume a desired shape once subjected to an operating load. In addition, the hydroelastic behaviour of the propeller blades is a potential source of excitation to the drivetrain.

Different approaches have been applied for hydro-elastic analyses of propellers. Most common methods are Computational Fluid Dynamics (CFD), Boundary Element

Methods (BEM) and a Vortex Lattice Methods (VLM), see for example Maljaars et al. (2015), Young (2008) and Taketani et al. (2013).

This study presents hydro-elastic analysis of a marine propeller under operational loading by two-way CFD/FEM based FSI co-simulation. The case of study was the quasi-static elastic response of propeller P1374 in a steady flow condition. Results were validated against experimental data.

## 2 HYDRO-ELASTIC ANALYSIS METHODOLOGY

The interaction of the structural and the fluid dynamics code was realised with the code independent coupling interface MpCCI. MpCCI is an application independent interface tool for the coupling of different simulation codes for multi-physical simulations. MpCCI manages the necessary data exchanges between the coupled codes. The systems under consideration are known as coupled systems. A coupled system consists of two or more distinct systems. Each system is governed by a characteristic set of differential equations, but both systems share some variables.

To find a solution for a coupled problem, all governing equations, which can be combined in a large system, must be solved simultaneously. This specific method is called strong coupling. However, solving a system with strong coupling is often difficult as different approaches are necessary to solve the sub-problems. An alternative approach is through weak coupling. In this partitioned approach, each problem is solved separately and during each time step, some variables are exchanged and inserted into the equations of the other problem. This procedure usually yields to a less exact solution compared to strong coupling. The advantages of the weak coupling are that the sub-problems can be solved faster than the complete system and that specialized solvers can be used for each. Overview of the simulation process used is presented in Figure 1.

In a fluid-structure interaction (FSI) simulation, the structure deforms due to forces caused by a fluid flow

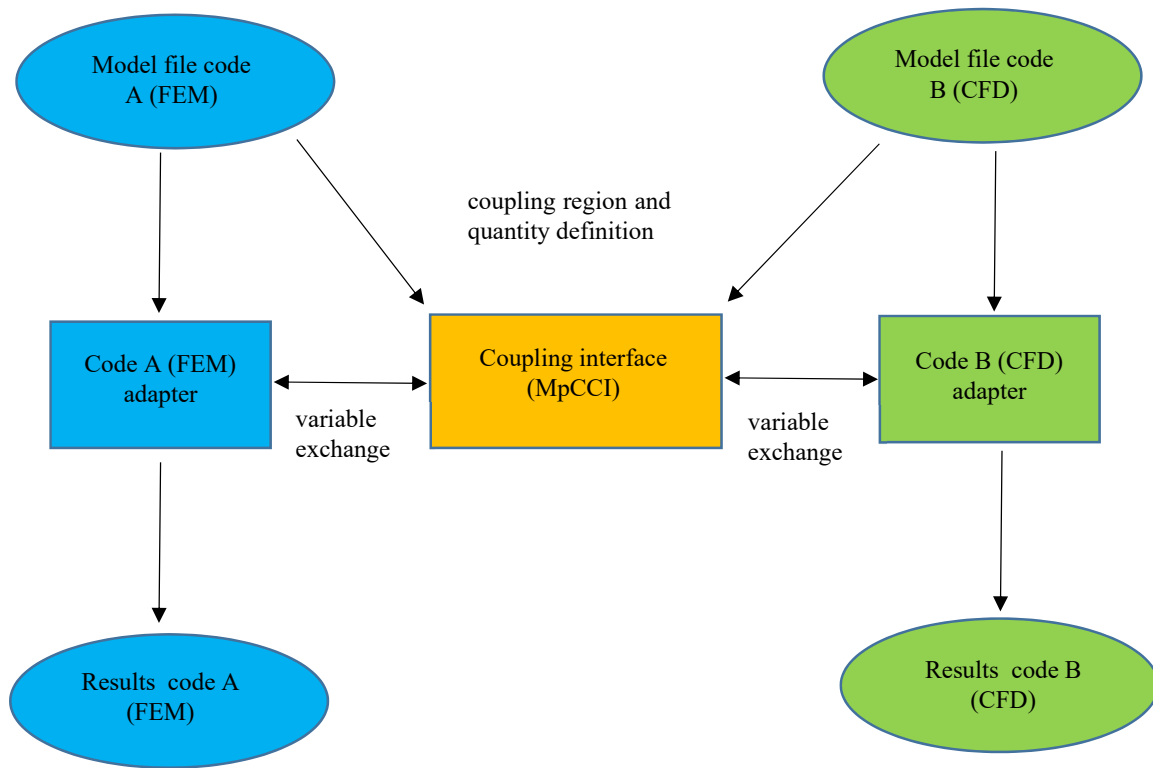


**Figure 1** Overview of the co-simulation process.

while the deformation changes the fluid boundary. The deformation (nodal displacements) must be transferred to the fluid mechanics code, while the forces (pressure) are sent from fluid mechanics code to the structural code.

Deformation, stresses and strains of structures were computed using the Finite Element Method (FEM). Solid mechanics code used was Abaqus (6.13-2).

Governing equations of fluid dynamics (Navier-Stokes equations and the continuum hypothesis) were solved numerically using finite volume method. CFD method was used to solve Reynolds-averaged Navier Stokes (RANS) equations. Fluid mechanics code used was Fluent (14.5.7).

### 3 CASE DESCRIPTION

The goal of this study was to analyze the propeller quasi-static elastic response under loading, and its effect on propeller hydrodynamic characteristics by carrying out two-way FSI co-simulation. The propeller used was open geometry propeller P1374 designed by MARINTEK for the purpose of having a propeller which could be used for experiments and validations of numerical tools in projects concerned with the dynamics of thrusters. The propeller diameter was 250 mm and the number of blades was 4.

Experimental data of two propellers with the same geometry was available (Savio 2015). The first propeller was manufactured in plastic material so that the deflections of the blades induced by the load were large enough to be measured by the optical system during experiments. The plastic propeller was manufactured by 3D printing

(material type was Rigid Opaque photopolymer, Savio 2015). The second propeller was manufactured in aluminum and therefore it was possible to compare the open water characteristics of the deformable and non-deformable propellers. Propeller deflections had been measured by means of stereo imaging applying 3D tracking technique, i.e. the position of a point in the three dimensional space was obtained by the knowledge of its projection on the two imaging planes forming the stereo system. Deflections of one of the blades of the propeller had been measured by tracking the displacements from a reference condition of a set of markers placed on the blade surface. Displacements had been computed as Euclidean distances between the locations of the markers in the deflected and non-deflected case. The locations of the markers had been determined from the stereo images through triangulation (Savio 2015).

#### 3.1 CFD model

A CFD-model was created based on geometry of P1374 propeller provided by Marintek. The water domain was modelled as a viscid fluid. Cavitation was not taken into account in the analyses. Calculation was performed with a steady analysis for one blade based on cyclic symmetry boundary conditions. A rotating reference frame method was used. The outer boundary of the computational domain extended 2.5xD in radial direction, 5.5xD in upstream direction and 8xD in downstream direction. Boundary conditions were set to simulate the flow around a rotating propeller in open water. Uniform velocity stream was used for inlet boundary condition and zero-pressure boundary

condition for outlet surface. Rigid wall boundary condition was used for the outer boundary.

The turbulence model used was a transition-sensitive three-equation  $k\text{-kl-}\omega$  model. A unstructured tetrahedron/prism mesh was used, including in total about 9.9 million cells. Growing prismatic cells from propeller and hub surfaces were used in the boundary layer. The thickness of the first layer of the boundary was  $10\ \mu\text{m}$ . The boundary included totally 23 layers. The remaining region in the domain was filled with tetrahedral cells, see Figure 2.

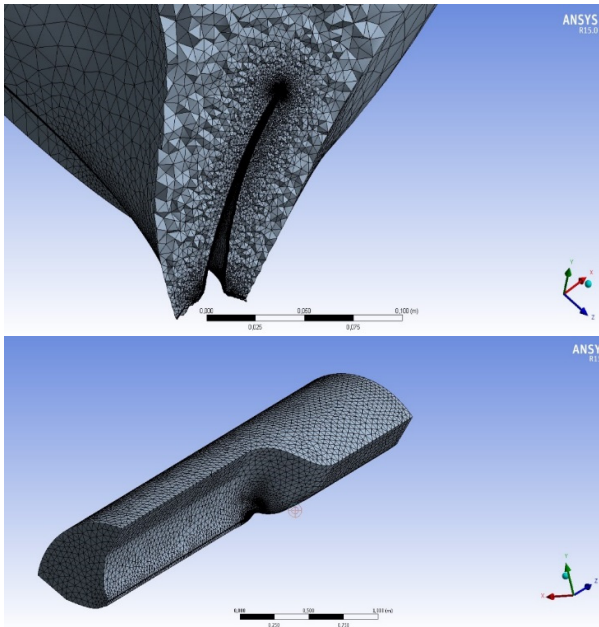


Figure 2 Unstructured CFD mesh

### 3.2 Structural model

The structural FE-model was created by using second-order continuum tetrahedral elements. In order to ensure that the results of the analysis are not affected by the density of the mesh, the mesh convergence was checked by using uniform pressure on the other side of the blade surface and calculating blade displacements with different mesh densities. The mesh was refined until additional refinement did not affect remarkably the calculated displacements. In addition, because the CFD mesh was very dense at edges of the blade, the FE-mesh was refined at these regions in order to get better spatial variable mapping between CFD and FE-models. The FE-model included about 370000 elements and 1700000 DOFs.

Material model used was linear elastic, because maximum stresses due to loads applied are relatively small, below 10 MPa. Young's modulus according to material supplier should be between 2000-3000 MPa and Poisson ratio 0.41. For first analyses value for Young's modulus of 2500 MPa was used. Structural model is shown in Figure 3.

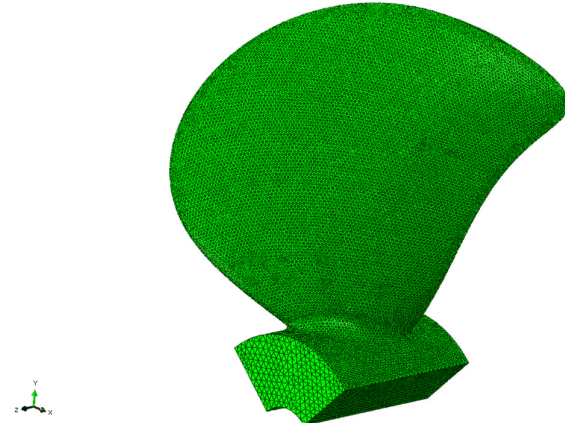


Figure 3 Structural FE-model

### 3.3 FSI Coupling

The meshes of the CFD and FE models at the coupling surface were non-conforming, i. e. the meshes of each subsystem were defined to optimize the solution of the subsystem. A shape function mapping was used for data exchange between two non-matching grids, which simply interpolates a variable field using the shape functions.

A quasi-static explicit steady-state coupling scheme applying two-way data transfer after each coupling steps was used. The data was transferred between the codes in both directions. A sequential serial coupling algorithm scheme used in co-simulation is presented in Figure 4. Code A is solid mechanics code (Abaqus) and code B is CFD code (Fluent). Dotted arrows in the figure represents data exchange between codes. Dotted arrows no 1, 5 and 9 represents pressure data transfer from CFD-code to FE-code and dotted arrows 3 and 7 represents displacement data transfer from FE-code to CFD-code.

A subcycling for CFD-code was applied. The idea of subcycling is the definition of extra iteration steps inside a coupling step. Motivation for subcycling is enabling optimal iteration settings for each solver concerning computational costs, stability and accuracy. Because CFD code required much more iterations compared with FE-code, 500 iterations without coupling and data transfer was used for CFD-code. The subcycling took place in the coupling scheme at the CFD solution steps, which are marked by 4, 8, ...etc in the figure.

Mesh smoothing was used for the CFD mesh to adjust the mesh of a zone with a deforming boundary (propeller blade surface). The mesh smoothing allows the interior nodes of the mesh to move, but the number of nodes and their connectivity does not change. In this way, the interior nodes "absorb" the movement of the boundary. Spring-based smoothing method was used in this case.

The FSI simulation was carried out for one operating point, for  $J=0.49$  at 7 rps. The simulation was performed iteratively until deformation and propeller characteristics

were converged. The propeller characteristics and deformation converged after approximately 6 coupling steps.

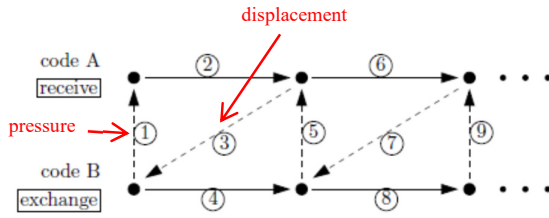


**Figure 4** Serial coupling configuration. Code A is solid mechanics code (Abaqus) and code B is CFD code (Fluent). Both codes exchange the data before iteration. Dotted lines (arrows) represents data exchange between codes.

#### 4 RESULTS

At the first stage, the open water global quantities computed by CFD-model alone (infinitely rigid propeller) were confirmed by comparing the  $K_T$ - $K_Q$  curves with the experimental curves. The non-dimension values used in the results are defined by equations (1)-(3), where  $\rho$  is water density,  $D$  [m] is propeller diameter,  $V_A$  is the water speed,  $n$  the propeller speed,  $T$  the propeller thrust and  $Q$  the propeller torque.

$$J = \frac{V_A}{nD} \quad \text{Advance coefficient} \quad (1)$$

$$K_T = \frac{T}{\rho n^2 D^4} \quad \text{Propeller thrust coefficient} \quad (2)$$

$$K_Q = \frac{Q}{\rho n^2 D^5} \quad \text{Propeller torque coefficient} \quad (3)$$

The experimental values in this case have been measured with non-deformable propeller (aluminum propeller). The results are shown in Figure 5. Satisfactory agreement was found, as can be seen.

The pressure distribution after deformation of plastic propeller is shown in Figure 6. The calculated blade deflection magnitudes are shown in Figure 7. Comparison of measured and calculated blade deflection distributions are presented in Figure 8.

Variation of Young's modulus can have significant effect on the blade deformations. The measured plastic propeller was manufactured by 3D printing (Savio 2015). Because 3D printing method can have potentially impact for example on material properties of 3D printed parts (homogeneity, anisotropy, dependency on printing direction, material defects, etc), it was decided to carry out simulations using two different Young's modulus, 1500 MPa and 2500 MPa. Comparisons of measured and simulated blade deflections are presented in Figure 9 and Figure 10.

As can be found, orders of magnitudes of displacements correspond the measured ones. However, simulated twist of the blade is smaller than the measured one. Comparisons of performance coefficients for aluminum and plastic propellers are shown in Figure 11. Results shows that even the thrust and torque coefficients itself can be estimated well, simulated modifications to the performance characteristics are smaller than measured ones. This is evidently caused by smaller blade twist in the calculations.

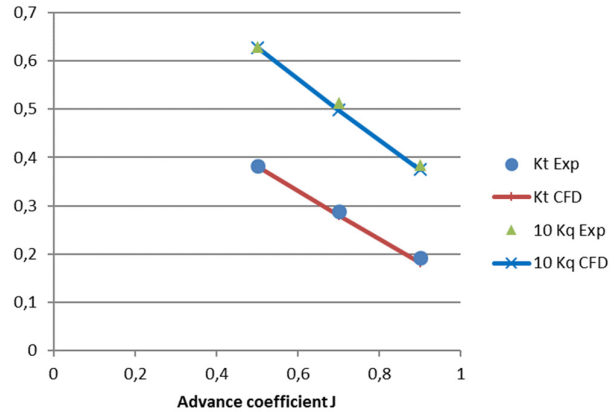


**Figure 5** Open water  $K_T$ - $K_Q$  curves computed for undeformed propeller. Index "Exp" refers to the experimental values. Rotating speed for both experimental and computational values was 11 rps

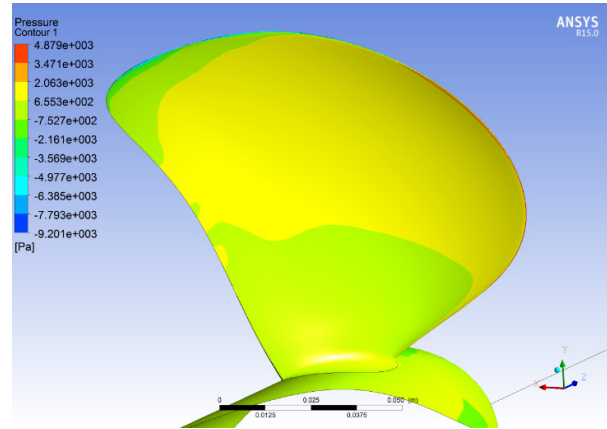


**Figure 6** Pressure distribution after deformation of plastic propeller

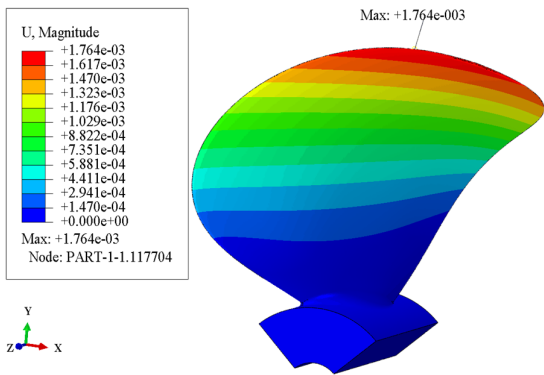


**Figure 7** Simulated blade deformation magnitudes for  $J=0.49$  at 7 rps. ( $E=1500$  MPa)

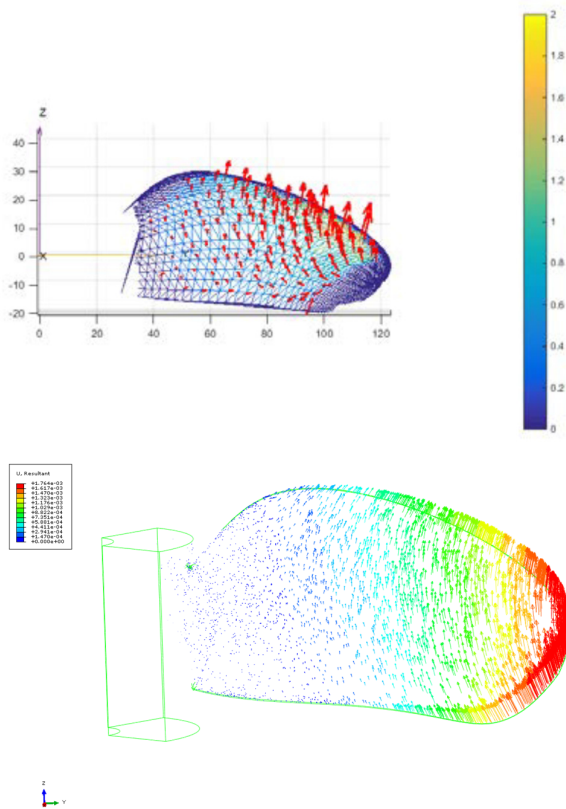


**Figure 8** Blade deflection vectors for  $J=0.49$  at 7 rps; measured (top) (Savio 2015) and calculated (bottom). ( $E=1500$  MPa)

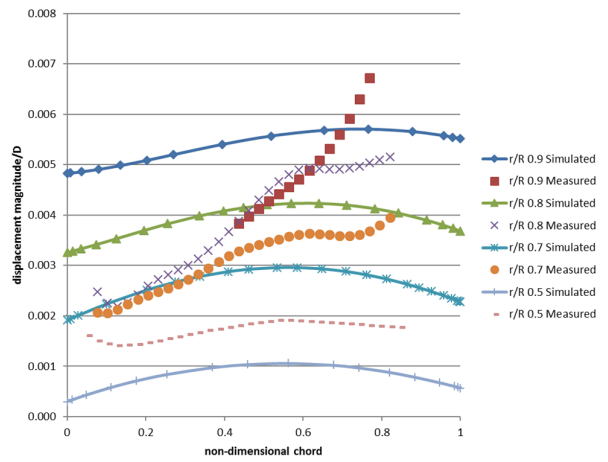


**Figure 9** Comparison of blade deflections for  $J=0.49$  at 7 rps. Young's modulus of the material used is 1500 MPa.  $R$  is propeller radius and  $r$  is radial distance from the hub. ( $0$ = trailing edge for non-dimensional chord)

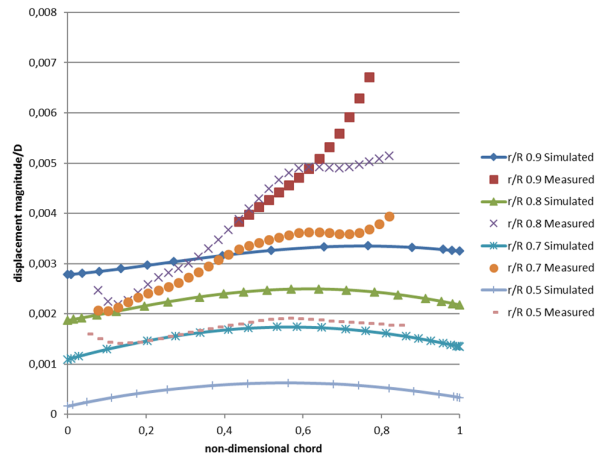


**Figure 10** Comparison of blade deflections for  $J=0.49$  at 7 rps. Young's modulus of the material used is 2500 MPa.  $R$  is propeller radius and  $r$  is radial distance from the hub. ( $0$ =trailing edge for non-dimensional chord)

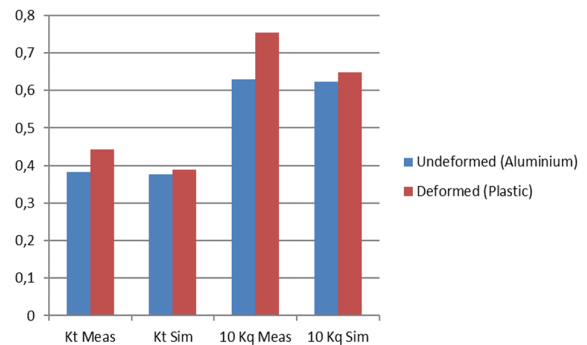


**Figure 11** Comparison of performance coefficients for aluminum and plastic propellers for  $J=0.49$  at 7 rps ( $E=1500$  MPa).

## 5 CONCLUSIONS AND SUMMARY

Two-way FSI co-simulation with Fluent CFD-code and Abaqus structural FE-code utilizing MpCCI was applied successfully.

Agreement between calculated and measured thrust and torque coefficient estimates itself was good. Order of magnitude of blade displacements correspond the measured ones. However, simulated twist of the blade is smaller than the measured one. Also simulated modifications to the performance characteristics are smaller than measured ones. This is evidently caused by smaller blade twist in the simulations. A possible reason for this can be the uncertainties in material properties of the blade. The measured propeller had been 3D-printed in plastic, which may have impact for example on the homogeneity, non-linearity and anisotropy of the printed material. It may also produce material defects inside the part. The blade deformations (blade twist) caused by fluid-structure interaction can be sensitive to the potential inhomogeneity of the blade material.

Concerning numerical accuracy, we do not expect the uncertainty to be large for the FEM computations since the mesh (built by second order elements) is much denser than those used in ordinary practice. The reason for this is that we wanted to get better spatial variable mapping between the hydrodynamic and mechanical grids, requiring the latter much finer grid. In addition, impact of FE mesh refinement for numerical accuracy was checked by mesh convergence check. Regarding RANS simulations, the use of a 9.9 millions cell mesh should also be enough for the open water performance as the good correlation with experiments for the non-deformed propeller suggests. However, even global forces were predicted relatively accurately, it is always possible that simulated pressure distributions may contain uncertainties. Therefore numerical uncertainty study for the hydrodynamic model also would be interesting.

In the future it is recommended to verify flexibility of the plastic blade by making static experiments by applying controlled force on the blade and measuring blade deflections (blade bending and especially blade twist). This experimental force-displacement relationship data enables validation of structural model, i.e. possible differences in material properties and also possible geometry imperfections (blade thickness, shape etc.) caused by 3D printing method. It is also recommended that FSI simulations will be carried out for several other operating points in order to get more data for simulation validation.

## ACKNOWLEDGMENTS

This research was funded by the EU MARTEC project HyDynPro. We are grateful to the research partners and funding institutions for their interest in this work. The authors are grateful to MARINTEK for providing the geometry and the test data of propeller P1374.

## REFERENCES

- Savio, Luca (2015). "Measurements of the deflection of a flexible propeller blade by means of stereo imaging", Fourth International Symposium on Marine Propulsors smp15, Austin, Texas, USA
- Maljaars, Pieter J., Kaminski, Mirek L. (2015). "Hydro-elastic Analysis of Flexible Propellers: An Overview", Fourth International Symposium on Marine Propulsors smp'15, Austin, Texas, USA
- Young, Y.L. (2008). "Fluid-Structure Interaction Analysis of Flexible Composite Marine Propellers," Journal of Fluids and Structures, 24, 799-818.
- Taketani, T., Kimura, K., Ando, S. and Yamamoto, K. (2013). "Study on Performance of a Ship Propeller Using a Composite Material," Third International Symposium on Marine Propulsors, Launceston, Tasmania, Australia.